PRINT ISSN 1119-8362
Electronic ISSN 2659-1502

Full-text Available Online at
https://www.ajol.info/index.php/jasem
https://www.bioline.org.br/ja

J. Appl. Sci. Environ. Manage.
Vol. 27 (11) 2597-2610 November 2023

Effects of Fly Ash on Compressive Strength and Durability Properties of Lean Concrete

***OHWOFASA, JO; IKUMAPAYI, CM; ARUM, C**

Department of Civil and Environmental Engineering, Federal University of Technology, Akure, Ondo State, Nigeria

**Corresponding Author Email: ohwofasacve152319@futa.edu.ng*
Co-Author Email: cmikumapayi@futa.edu.ng; carum@futa.edu.ng

ABSTRACT: Concrete production and waste generation are among human activities that negatively impact the environment. This study investigated the effects of fly ash on compressive strength and durability properties of lean concrete using appropriate standard methods. The results showed that the compressive strength of the control mix is higher than those of fly ash concrete mixes. The compressive strength of the fly ash blended mixes decreased as the replacement level increased. However, the strength increased with hydration time, and the optimal replacement level being 5%. While the chloride ion penetration and water absorption rate decreased, the sulfate resistance increased with hydration time and replacement level. The fly ash mixes exhibited better durability properties than the control mix in all durability tests conducted. The SEM-EDX analysis showed that mixes with well-packed microstructures exhibited favorable compressive and durability properties. In conclusion, Class C fly ash is recommended for lean concrete mixes at a replacement level of up to 15% when compressive strength is the primary concern, while mixes with a replacement level of 25% or more are recommended in areas susceptible to sulfate attack.

DOI: https://dx.doi.org/10.4314/jasem.v27i11.32

Cite this paper as: OHWOFASA, J. O; IKUMAPAYI, C. M; ARUM, C. (2023). Effects of Fly Ash on Compressive Strength and Durability Properties of Lean Concrete. *J. Appl. Sci. Environ. Manage.* 27 (11) 2597-2610

Dates: Received: 30 September 2023; Revised: 29 October 2023; Accepted: 07 November 2023 Published: 30 November 2023

Keywords: compressive strength; durability of concrete; fly ash replacement; lean concrete; water absorption.

INTRODUCTION

Concrete, in essence, is a versatile material that can be formed into different shapes, and is widely used for construction activities all over the world as it gives a good durability properties to the structures which it forms. In addition, concrete consist majorly of inert materials (such as coarse and fine aggregates) and cement paste which act as the binder (Ikumapayi, 2018). The problems associated with the production processes of the constituents of concrete, which include the emission of toxic gases, high energy and natural resources consumption, pose severe effects on the ecology and the economy of a country (Wilińska and Pacewska, 2018). In order to conserve the environment from solid industrial, domestic, agricultural waste, and the likes, ordinary Portland cement OPC should be partially replaced with pozzolans or supplementary cementitious materials like rice husk ash, fly-ash, corncob ash, millet husk ash, periwinkle shell ash (Ikumapayi, 2017). The substitution of fly ash in concrete production helps mitigate these aforementioned problems and reduces the cost associated with the fly ash disposal. However, despite the ecological and economic benefits derived in partial replacement of cement with fly-ash in concrete production, the strength and durability properties of the concrete is considerably compromised; as such, the amount of substitution made should be controlled (Saha, 2018). In recent time, the durability of concrete has been a focal point of researchers in concrete field, especially marine structures (Zhang and Xi, 2016). Durability is a concrete property that defines its resistance to deterioration processes resulting from weather action, abrasion and chemical attack, *etc.* (Jemimah and

Prince, 2019). According to Nath and Sarker (Nath and Sarker, 2011), in a severe environment, the service life of a structure depends on the durability of the concrete from which it is formed. To maintain the service life of marine structures like bridges, jetties, wharf and the likes, against adverse environmental effects, the chloride ion ingression must be reduced. Corrosion of steel bars caused by the penetration of chloride ion results in volume change; which leads to cracks, spalling of the concrete, and a weakening of its load-carrying capacity and bonding with the steel (Ikumapayi, 2019). Jaya (Jaya, 2020) submits that compressive strength is the most important test of all concrete tests. It defines the concrete's ability to sustain loads causing failure. The compressive strength of concrete varies with the intended use of the structure. It depends on the mix ratio, the properties of the constituent materials, the water-cement ratio, and curing. The diverse modes in which solid wastes is incorporated into concrete production has been of interest to researchers. This is with the view to reducing greenhouse gas emissions and the cost in waste disposal, conserve energy, protecting natural resources, and not compromising the standard of concrete. Fly ash is a by-product of combusted coal which contains siliceous and aluminous properties that forms cementitious compound when mixed with water and lime (Pati *et al*., 2003). The use of fly ash in concrete works, improves its workability, reduces concrete defects, improves compressive strength, reduces permeability, and increases resistance to chemical attack in severe environment (Demir *et al*., 2018). Furthermore, substituting fly ash products into concrete reduces construction costs and improves its physical and durability properties. Due to the low permeability property of fly ash, the cracks associated with corrosion of reinforcing bars caused by chemical attack (sulfate, and chloride ion penetration) in concrete are less likely to occur (Sumer, 2012). Lean concrete is a less strong and less expensive concrete with a high aggregate content and a low cement content. It is used in non-load-bearing applications such as blinding under foundations, pipelines huanching, and mass concrete use in dams (Al-Modern *et al*., 2018). Little or no work has been done on the investigation of the use of fly ash in low-strength concrete production, which is mostly used as a blinding course in civil engineering operations. Most studies on binary blends (a pozzolan and cement mix) of fly ash with cement deals greatly on either the mechanical and durability properties of the geopolymer concrete with high strength grades. More so, other studies cover only a few replacement gaps with outrageous replacement steps and few testing days. Therefore, this study serves as an effort to bridge the drawbacks of previous studies by investigating both the strength of low-grade concrete and its durability properties over a larger replacement range, with smaller replacement steps and longer testing days. The objective of this paper was to evaluate the effects of fly ash on compressive strength and durability properties of lean concrete.

MATERIALS AND METHOD

Materials: The materials used for this study are shown in Figure 1. These materials were sourced locally and tested to ensure that they meet all the necessary standards. Dangote Portland limestone cement (PLC), CEM II 32.5R (B-L), was used as the main binder for concrete mixing. The cement conforms with the specifications laid by British Standards - (BS EN197-1, 2011). Fly ash from Itobe, Kogi State, Nigeria was obtained by burning coal at a temperature of 850°C.The portion of Fly ash finer than sieve No 325 were used. The chemical compositions of the fly ash and cement are shown in Tables 1 and 2 respectively.

Figure 1. Materials used in concrete production.

Table 1. Chemical composition of the fly ash.

Oxides (%)	Fly Ash
SiO2	35.04
$Al2O_3$	14.04
Fe_2O_3	6.76
CaO	22.8
MgO	4.56
SO_3	3.25
TiO_2	1.6
LOI	3.86
$SiO_2+Al_2O_3+Fe_2O_3$	55.84

Based on American Society for Testing and Materials Standards - (ASTM C618, 2019), the fly ash is Class C since the sum of the SiO_2, Al_2O_3, and FeO_3 is less than 70%. The Bogue composition of the respective compounds (Tricalcium silicate (C_3S), dicalcium silicate (C_2S), Tricalcium aluminate (C_3A), and tetracalcium aluminoferrite (C_4AF)) in Portland cement shown in Table 2 are obtained using Equation 1 to 4 respectively.

Table 2. Elemental oxides composition of cement as per specified standard

Compound (elemental oxides) of OPC	% composition obtained from XRF analysis	Required Limit for CEM II Portland composite cement as per BS EN 197-1:2011 and BS 12:1997 (%)	Remarks
SiO_2	19.49	17.46 - 21.59	Within limit
Al_2O_3	4.28	3.29 - 6.14	Within limit
Fe_2O_3	3.16	1.21 - 3.76	Within limit
CaO	63.04	58.67 - 63.9	Within limit
MgO	1.46	0.61 - 3.30	Within limit
SO_3	1.28	< 3.5	Within limit
Na_2O	0.11		
K_2O	0.13		
$K_2O + Na_2O$	0.24	< 2.0	Within limit
C_3S	69.63	50 - 70	Within limit
C_2S	3.70	15 - 30	Below limit
C_3A	6.01	5 to 10	Within limit
C_4AF	9.60	5 to 15	Within limit

$$C_3S = 4.07C - 7.60S - 6.72A - 1.43F - 2.85\ S^* \quad 1$$

Where: C represents the percentage of calcium oxide (CaO); S represents the percentage of silicon dioxide (SiO_2);
A represents aluminum oxide (Al_2O_3) F represents the percentage of ferric oxide (Fe_2O_3); and S^* represents sulphur trioxide (SO_3).

$$C_2S = 2.87S - 0.75\ (C3S) \quad 2$$
$$C_3A = 2.65A - 1.69F \quad 3$$
$$C_4AF = 3.04F \quad 4$$

The Bogue composition of cement compounds is only valid when the ratio of alumina (A) to ferrite (F) is greater than or equal to 0.64 (Nwokocha and Munachiso, 2022). The physical properties of the binder are shown in Table 3. British Standards - (BS EN 196-6, 2018) states that a good cement (binder) must not have more than 10% of its total weight retained in the 90 micron sieve, according to its fineness requirement. The test results show a satisfactory outcome except for the 40% replacement level, which had a fineness value of 11.1, exceeding the value specified in the code. Also, the length increase observed during the soundness test of the binders not exceed 10mm indicating that all the blends are sound.

Table 3. Physical properties of the binders

Cem. (%)	FA (%)	Fineness %) *sieving method*	Soundness (mm) *Le Chatelier*	Consistency (%)	Initial Setting Time (mins)	Final Setting Time (mins)
100	0	0. 6	1	26	82	402
95	5	2.2	0.5	26	96	432
90	10	4.2	0.5	24	150	491
85	15	5.9	1	23	184	567
80	20	6.6	1	23	223	615
75	25	7.4	1	23	258	649
70	30	8.4	1	23	301	674
65	35	9	1	23	336	733
60	40	11.1	2	23	378	772

The initial and final setting time of the binders is are shown in figure 2. The paste with 0% to 15% replacement of fly ash falls within the recommended 10 hour final setting time range, while the blends with 20% to 40% replacement levels exceed the final setting time in specifications. Siddique (2004); Rukzon and Chindaprasirt (2014), reported similar trends in final setting time of pozzolan-cement binder. The water requirement of the standard consistency tests of the binders was observed to decrease from 26% to 23% as the percentage level of fly ash increases. The aggregates used for this study are fine and coarse aggregate. The fine aggregate was obtained from river Ogbese (Nigeria), having sizes ranging from 150 microns to 4.75mm. The coarse aggregate (granite) of 12.5mm size was used for this study. The granite was obtained from JCC quarry plant along Owo Road, Ondo State; and it is consistent with the provisions of the standard specification for concrete aggregates described by American Society for Testing and Materials Standards - (ASTM C33/C33M, 2018). The physical properties of the aggregates are shown in Table 4.

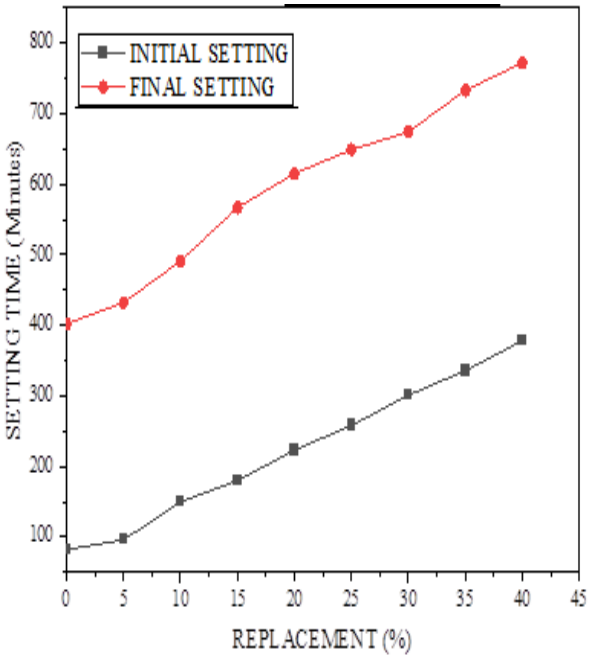

Fig 2. Initial and final setting time of cement-fly ash blended paste

The test results were obtained in accordance with specification (ASTM C136, 2006; ASTM C29/C29M, 2016; ASTM D2487, 2017; BS 812-109, 1990; BS 812-110, 1990; BS 812-112, 1990; BS EN 1097-6, 1995). The particle size distribution of the fine aggregate is shown in Figure 3; and based on the value of coefficient of curvature and curve shape, the sand is considered to be well graded.

Table 4. Physical properties of the aggregates

Test	Aggregates	
	Sand	Granite
Moisture content (%)	1.35	
Specific gravity	2.68	2.61
Aggregate impact value (%)		15.33
Aggregate crushing value (%)		22.12
Bulk Density (kg/m³)	1645	1597
Fineness Modulus	3.69	
Coefficient of Uniformity, Cu	3.56	
Coefficient of Curvature, Cc	1.19	

The fineness modulus shows that the aggregate is coarse sand. The coefficient of curvature and uniformity is obtained from Equation 5 and 6 respectively. Potable water obtained from a borehole within the campus of the Federal University of Technology Akure, Nigeria, was used for mixing the concrete. It was ensured that the water fully satisfy the requirements of concrete mixing water as specified in British standard code British Standards - (BS EN 1008, 2002).

$$Cc = \frac{D30^2}{D60\ X\ D10} \qquad 5$$

$$Cu = \frac{D60}{D10} \qquad 6$$

Where; D_{60} represent the diameter for which 60% is finer, D_{10} represent the diameter for which 10% is finer, and D_{30} represent the diameter for which 30% is finer. From Figure 2, D_{60} =0.57, D_{30} =0.33, and D_{10} =0.16

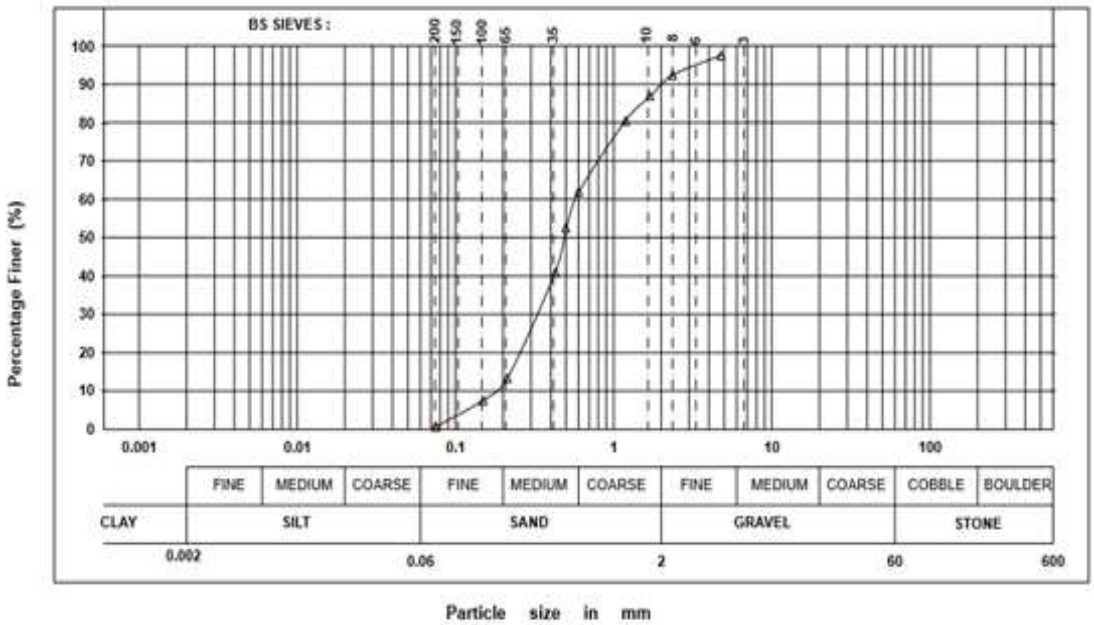

Fig 3. Particle size distribution of fine aggregate

Mix design: The compressive strength and durability properties of fly ash blended lean concrete was investigated. Portland limestone cement was partially replaced with class C fly ash, in a replacement range of 5% to 40% at a 5% step size increment. A total of 405 cylindrical test specimens were produced using mix ratio 1:4:8, and a constant water-binder ratio of 0.7.

Preparation, casting and curing of pozzolanic concrete: The materials were batched by weight, and the mixing was done manually. The concrete mixes were thoroughly mixed for 5 minutes each, until a smooth, even paste was formed. The workability of the plastic concrete was evaluated using the slump test and the compacting factor test and in accordance with British Standards - (BS 1881-103, 1993). For each replacement level and test day, three concrete samples with 100mm diameter and 200mm thickness were cast for the compressive strength test; while two concrete samples with 100mm diameter and 50mm thickness were cast for the durability test. The cast samples were left for 24 hours before being removed from its form and immersed in water. The concrete samples were cured (by immersion in water) at their respective ages (7, 14, 28, 56 and 90 days). However, concrete samples meant to assess the mass change of the fly-ash blended mix were cured in water for 28days, in sulfuric acid for the 60 days and ambient temperature for 365 days.

Test on hardened concrete: The compressive strength tests was carried using a Universal Compression Loading machine of Capacity 1000kN, and load application rate of 0.5MPa/s. At each test day, three cylindrical (100mm diameter and 200mm height) specimens from each mixes were tested and the average of these readings was taken as the compressive strength of that mix. The test was carried out according to the standard guidelines of American Society for Testing and Materials - (ASTM C 39, 2001). Figure 4 shows a schematic of the setup for the Rapid Chloride Penetration Test (RCPT). Two test samples (100mm diameter and 50mm height) were placed in RCPT migration cells with 3.0% NaCl solution (catholyte) and 0.3 N NaOH solutions (anolyte). A constant potential of 60 ± 0.1 V was applied on the concrete. The current readings were recorded at 30 min intervals for 6 H. The test was done for 7, 14, 28, 56, and 90 day and in accordance with American Society for Testing and Materials Standards - (ASTM C1202, 2012). The test specimens for determining the rate of water absorption were first conditioned in accordance with American Society for Testing and Materials Standards - (ASTM C1585, 2013). The test specimen (100mm in diameter and 50mm in height) was placed in an oven at 50 ± 2°C for 3days, after which it was removed and placed in a sealed container for 15 days. The curved surface area, and one end of the specimen was seal using epoxy paint and plastic sheet. The setup for the water absorption rate is shown in Figure 5. The initial mass and the masses of the samples after it was partially placed in water to a depth of 3mm at the specified time (0, 1, 5, 10, 20, 30, 60, 120, 180, 240, 300, 360, 420 min and 1, 2, 3, 4, 7, 8, 9 days) were recorded.

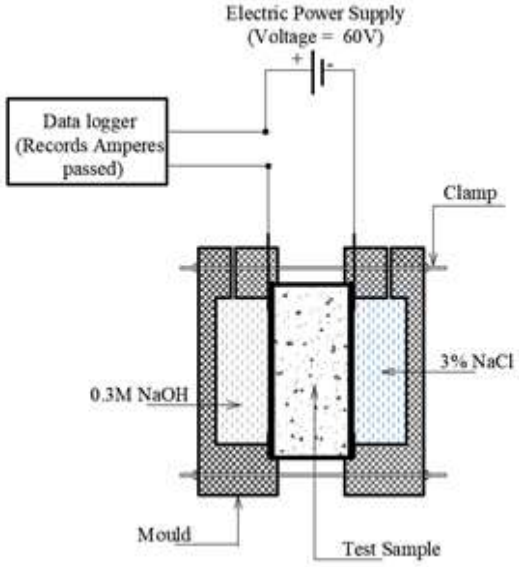

Fig 4. Rapid chloride penetration test (RCPT) setup

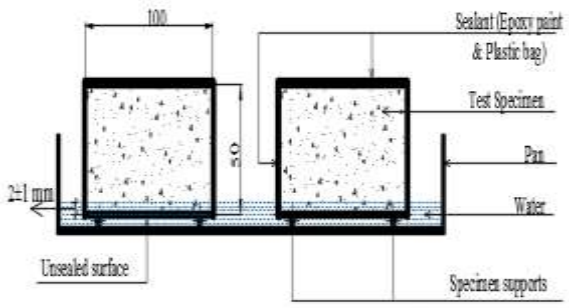

Fig 5. Setup for water absorption test

For mass change, the test specimens (100mm diameter and 50mm height) were first cured in water for 28 days, after which it was removed and its weight was measured as the initial mass. The samples were then cured in an acidic solution (5% of dilute sulphuric acid by volume of water with a pH maintained about 4) (Verapathran and Murthia, 2016). The samples were removed after 62 days from the solution and allowed to dry at room temperature for 24h; and the mass was recorded. The samples were further cured under ambient temperature for 365 days, after which the

mass was recorded. Samples of some test specimens at the different test age were analyzed by scanning electron microscopy (SEM) and energy dispersive x-ray (EDX).

RESULTS AND DISCUSSIONS

Fresh Concrete Properties: The slump and compacting factor test results are shown in Figure 6. All the mixes exhibited a true slump. Additionally, almost all of the slump values fall within the recommended range of 20 mm to 50 mm, which is suitable for mass concrete structures and pavements. The result for the compacting factor as recommended for satisfactory and usable concrete should range from 0.7 to 0.99. The test results show a compacting factor ranging between 0.93 and 0.98 for all replacement levels; thus, the mixes met the recommended requirement for satisfactory and usable concrete. Hence, it indicates that the concrete mixes are appropriate.

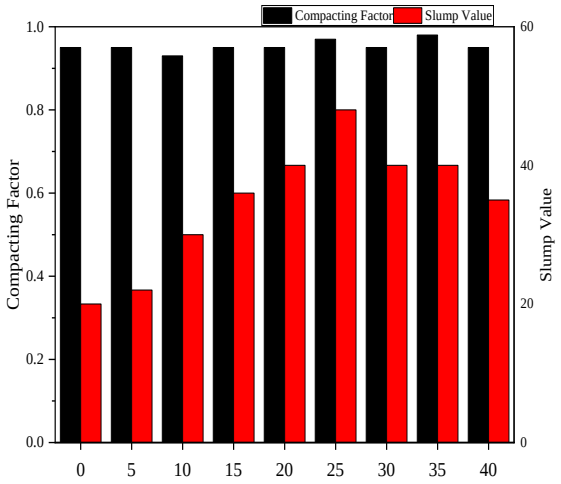

Fig 6. The compacting factor and slump value of the various concrete blends

Hardened Concrete Properties

Compressive strength: The compressive strength values of the test samples at the different test ages are shown in Figure 7. The compressive strength decreases with an increase in replacement level. The compressive strength of the concrete mixtures at 28 days varied from 2.3 to 7.4 mPa. The fly ash-blend concrete samples exhibited lower strength than the control concrete samples designed to achieve the same 28-day compressive strength. The control test samples exhibited the highest strength values on all curing days; but after 28 days of hydration, the rate of strength development was minimal (7.7mPa and 7.8mPa for 56 and 90 days, respectively) at the later days. On the other hand, the fly ash blended concrete initially had lower strength values but showed exponential increases on later curing days. Concrete mixes with 5% and 10% replacement gained 73% and 62% of the control concrete's strength at 28 days, respectively. At 90 days, the fly ash blended concrete with 5%, 10%, and 15% replacement gained 87%, 72%, and 68% of the control concrete's strength, respectively. Fly ash concretes with lower replacement levels showed higher strength gains at a later age than those with replacement levels greater than 20%. The trends in the strength development of the fly ash concretes are similar to those reported in the literature (Siddique, 2004). The microstructures of the samples tested for compressive strength on day 7 are shown in Figure 8. Calcium silicate hydrate (C-S-H) radiating crystals and fibrous ettringite crystals are widely distributed in the fly ash concrete. However, the ettringite is more pronounced in Figure 8A (the control mix) than in Figure 8B (fly ash concrete mix with a 10% replacement level).

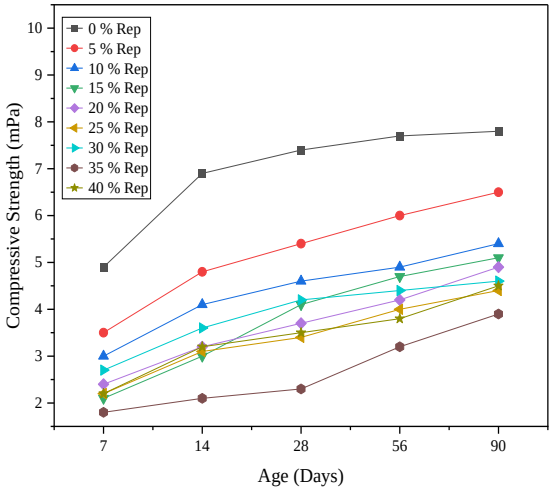

Figu 7. Compressive strength development

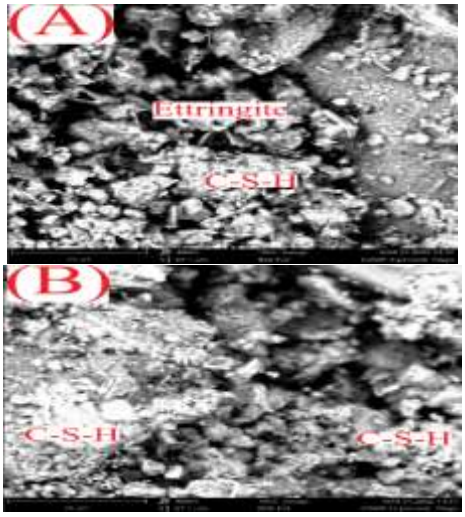

Fig 8. Scanning electron microscopy of concrete specimens used for compressive strength at day 7.

The densified structure of the control mix is evident in its compressive strength at an early curing age. Figures 9A and 9B show the SEM-EDX of samples (control mix and 10%) for compressive strength at day 28. The figures demonstrate a denser, amorphous gel-like structure with low porosity compared with those in the early days of curing. This amorphous gel fills the spaces between the concrete matrixes, thus reducing the pores. This reduction in pore spaces contributes to the improved compressive strength.

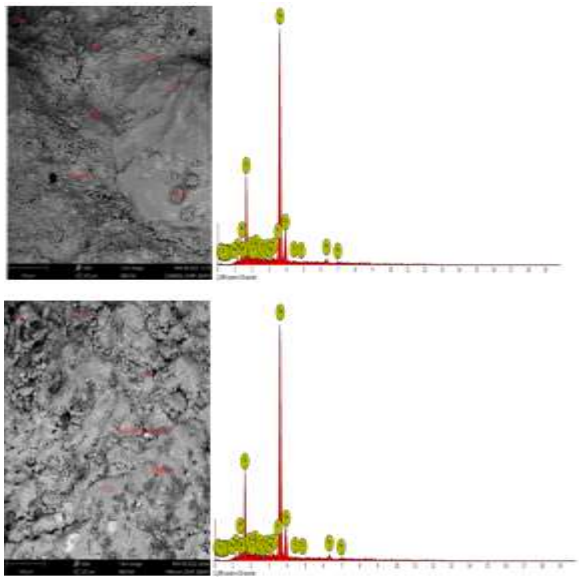

Fig 9. Scanning electron microscopy and energy dispersive x-ray of the control mix and fly ash concrete mix at day 28.

Figures 10A – 10C illustrate the SEM EDXS analysis on the compressive strength test of some selected mixes (control, 5%, and 20%). As the hydration time of the concrete mix cured in water increases up to 90 days, the matrix of the mixes becomes densified due to the hydration products that are formed. The dense structure of Figure 10A (control mix) and Figure 10B (5% replacement mix) are evident on both the compressive strength. Figure 10C shows the morphology of the 20% replacement mix, which has a porous microstructure that affects the strength result when compared to the control and 5% mixes. Also, the EDXS analysis shows it has the least Ca/Si ratio, hence has a higher degree of polymerization and the least dissolution of silica required to fill the available pores. The compressive strength appears to increase with decrease in the Na/Si ratio. Malkawi *et al.*, (2016) observed similar trend in a study on the effects of alkaline solution on properties of the high calcium fly ash geopolymer mortars.

Rapid chloride penetration: The penetration of chloride ions into concrete is dependent on the number of days of hydration. As shown in Figure 11, the longer the hydration days, the less permeable it becomes to chloride ions Penetration. While a moderate to high rate of chloride ion penetration were observed in all samples at day 7, the levels decreased to a range between low and moderate in the later curing days.

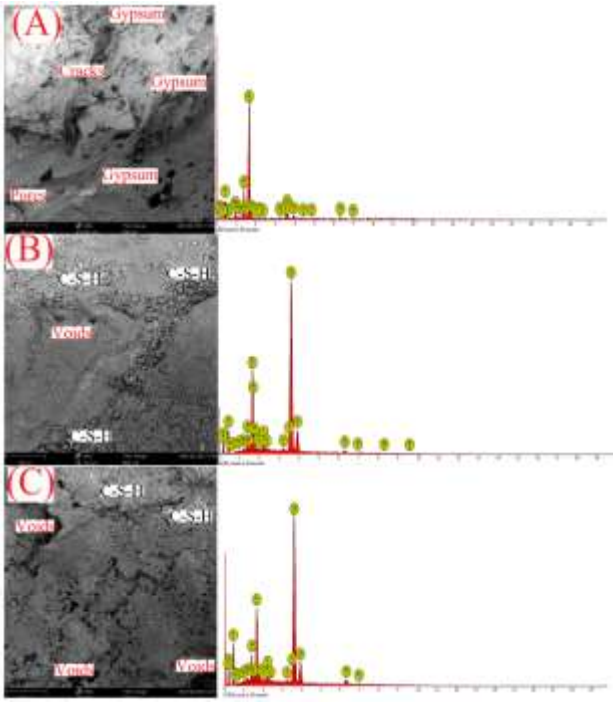

Fig 10. Scanning electron microscopy and energy dispersive x-ray of the control mix and fly ash concrete mix at day 90.

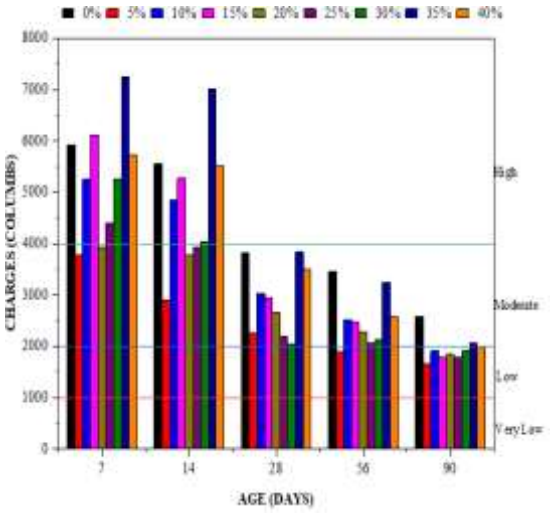

Fig 11. Rapid chloride penetration test of the concrete mixes

On day 7, the ion penetration rate was high for all samples, with charge values ranging from 3900 coulombs for 5% replacement to 7400 coulombs for 35% replacement. The ion penetration rate remained high on day 14, with charge values ranging from 3000

for 5% replacement to 7000 coulombs for 35% replacement. At day 28 and 56, the rate of chloride ion penetration for 35% replacement reduced drastically to 3834 and 3244 coulombs respectively. At these hydration days, almost all the samples have charge values within the moderate ratings. Furthermore, at day 56, all the blended mixes show improved ion penetration resistance compared to the control mix, with the 35% replacement mix slightly below the control mix. Overall, at day 90, most of the mixes with high replacement percentages that had low performance from the onset now exhibit high performance in resisting chloride ion. Mixes with 15%, 20%, 25%, 30%, 35%, and 40% replacement show improved performance of 72.2%, 53.1%, 47%, 63.8%, 71.4%, and 65.1% respectively when compared with their respective mixes at day 7.

The microstructures of some selected mixes used for RCPT at day 7 is shown in Figures 12. The 5% mix (Figure 12A) has a densified structure than the 40% mix (Figure 12B). This occurs from some pozzolanic activities when the fly ash mixes reacts with the undiluted excess calcium from the cement. The outcome is evident in its resistance to chloride ion on its early curing age as when compared with other mixes. The fibrous ettringite in this mixes are well pronounce; the salt and bases used for the test spiked the formation of these ettringites. Scanning electron microscopy of 20% replacement mix at day 28 is shown in Figure 13. The gel-like structure of this concrete mix helps in improving its resistance to chloride ions as it shows minute pore structures. With comparison to the mixes at day 7, the 20% replacement mix shows good resistance in the formation of fibrous ettringites; and this is associated with the longer hydration period.

Water absorption: The rate of water absorption for the respectively test days are shown in Figure 14. The rate was determined by plotting the amount of absorption (in millimeters) against the square root of the time (in seconds). A regression analysis was then used to fit a line to the data, and the slope of the line was used to calculate the rate of absorption. The slope of the regression line measures the rate of absorption, in $mm/s^{0.5}$ having a R^2 value of 0.98 that indicates a good relationship between the rate of absorption and time. The initial and secondary rates of absorption for all the concrete mixes at days 7, 14, 28, 56, and 90 are shown in Table 4 and Table 5 respectively. The initial rate of water absorption decreased with increasing hydration period. While the secondary rate of water absorption is a function of its initial rate. A higher initial rate of absorption gives a lower secondary rate of absorption, and the slope tends to increase steadily. Concrete with fly ash blends had a lower rate of water absorption than the control concrete mix. Among the fly ash concrete mixes, the 30% replacement mix designation demonstrated the lowest initial rate of absorption, while the 35% replacement mix had the lowest secondary rate of water absorption. The percentage decrease in the initial rate of water absorption for the 30% replacement mix at day 90, compared to day 7, was 74.2%. Similarly, the secondary rate of absorption for the 35% replacement mix decreased by 31.5%. Furthermore, after the 56 days of hydration, the secondary rate of absorption for concrete mix designations of 25%, and 40% decreased considerably.

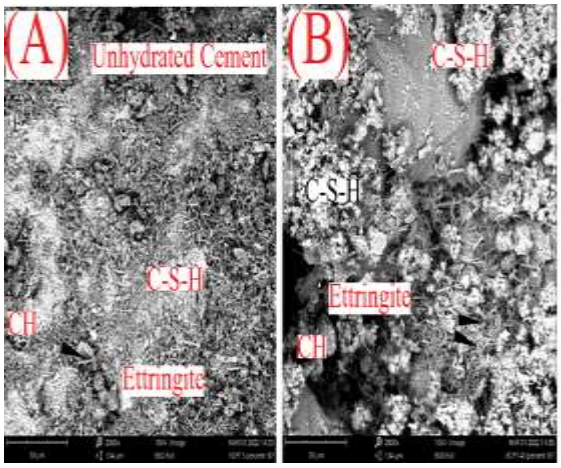

Fig. 12. Scanning electron microscopy of concrete specimens used for rapid chloride penetration test at day 7.

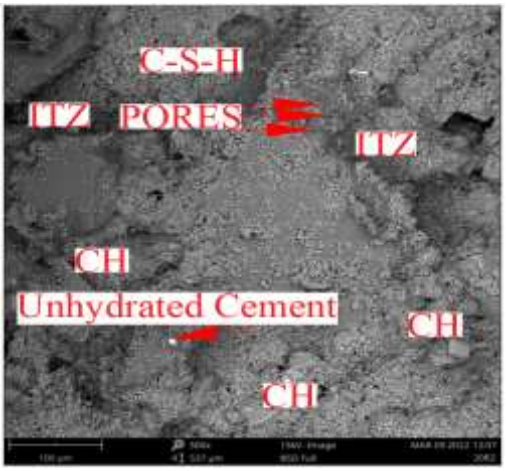

Fig 13. Scanning electron microscopy of concrete specimen used for rapid chloride penetration test at day 28.

The reduction in water absorption in the fly ash mixes can be attributed to the filler and pozzolanic effects, which enhanced the quality of the cementitious compound and contributed to its densification. The percentage reduction in the initial rate of water absorption of concrete exhibited a substantial increase with curing age, in contrast to the secondary rate of

water absorption that is dependent on the initial rate of absorption. These findings align with the research conducted by *(*Kotwa, 2015*;* Liu *et al.*, 2022).

Mass change: The percentage mass gain of the test samples is shown in Figure 15. In general, the mass change of the concrete mixes follows an increasing trend when cured in a 5% sulphuric acid solution, while it decreases under ambient conditions. The control mix exhibits the lowest mass gain at 0.17%. The mass gain increases gradually, reaching a peak of 0.73% at the 30% replacement level, before declining to 0.26% at the 40% replacement level. This observation aligns with the findings of (Dillard, 2021; Guo *et al*., 2021). Fly ash concrete mixes exposed to sulfate at an early age retard the hydration products and pozzolanic activities necessary for filling the available pores. The crystallization of the sulfuric acid solution is believed to occupy the pores of the concrete, leading to the observed mass gain. Under ambient conditions, the mass loss of the fly ash concrete mixes decreases with increasing replacement levels. The 25% replacement mix exhibits the least deterioration, with a weight loss 39.78% lower than that of the control mix. Beyond the 25% replacement mix, the weight loss slightly increases but dips again at the 40% replacement mix. The control mix experiences more mass loss (4.55%) compared to the blended mixes; with the 25% fly ash mix showing the least deterioration. The reduction in weight can be attributed to the re-concentration of sulfate solution, as well as the decomposition of calcium silicate hydrates and calcium hydrates. These outcomes align with the recommended range (between 20% and 75% replacement with high calcium fly ash) for substituting fly ash in concrete, as stated by (Liu *et al.*, 2018; Sudheen, 2008; von Fay, 1995). The SEM EDXS analysis on sulfate attack in some selected mixes (control, 25%, and 40%) is shown in Figure 16A–16C. Figure 16A shows more gypsum occupying the voids of the control mix than the 25% replacement and 40% replacement mixes in Figures 16B and 16C, respectively.

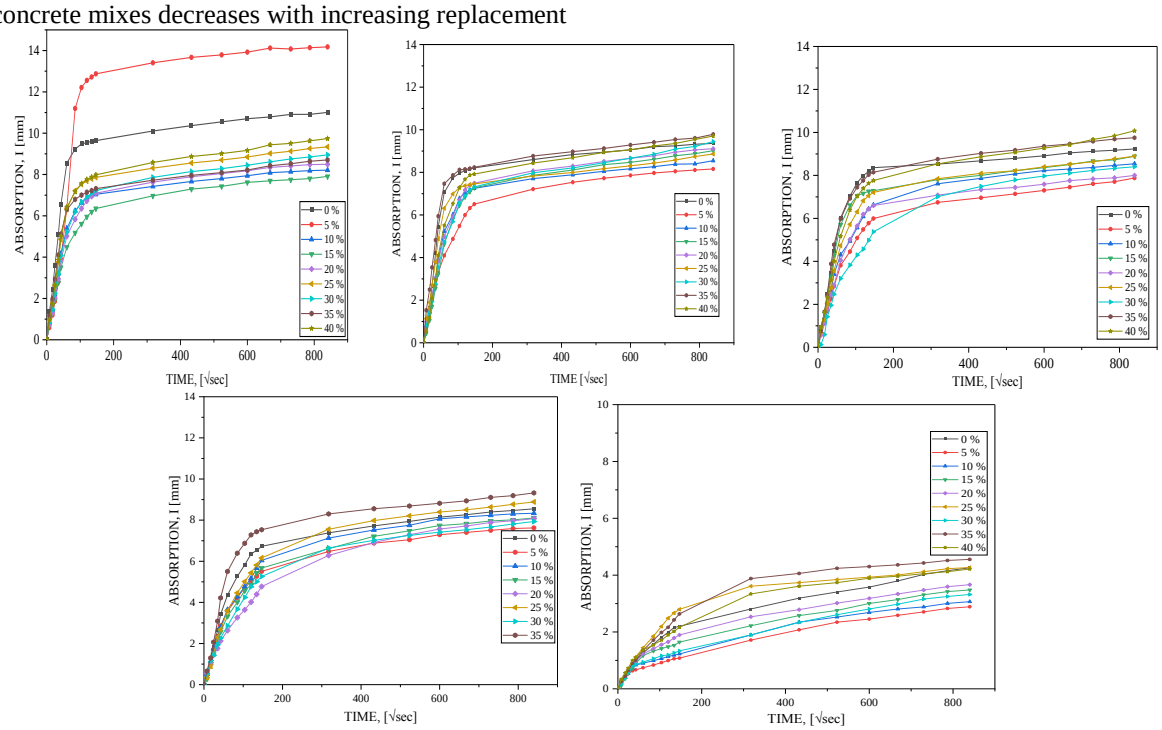

Fig 14. The rate of water absorption of concrete at day 7, 14, 28, 56, and 90.

Table 5. Initial rate of water absorption for the concrete mixes at all curing days (mm/s$^{0.5}$)

Replacement %	7days	14days	28days	56days	90days
0	0.1444	0.1228	0.101	0.0763	0.0234
5	0.1047	0.0697	0.0627	0.0612	0.0187
10	0.09197	0.0878	0.0716	0.0618	0.0197
15	0.0955	0.0788	0.0763	0.058	0.0203
20	0.0855	0.0823	0.0679	0.0435	0.0224
25	0.1073	0.1056	0.0796	0.0629	0.0241
30	0.0887	0.0785	0.0581	0.0474	0.0229
35	0.1243	0.1071	0.1047	0.095	0.0224
40	0.1096	0.0953	0.086	0.0695	0.0255

Table 5. Secondary rate of water absorption for the concrete mixes at all curing days ($mm/s^{0.5}$)

Replacement %	7days	14days	28days	56days	90days
0	0.0018	0.0013	0.0014	0.0022	0.0028
5	0.0014	0.0018	0.0022	0.0022	0.0022
10	0.0014	0.0016	0.0017	0.0023	0.0021
15	0.0021	0.0022	0.0015	0.0027	0.0025
20	0.0016	0.00204	0.0017	0.0033	0.0022
25	0.0017	0.002	0.002	0.0024	0.0013
30	0.0018	0.0028	0.0026	0.0023	0.0027
35	0.0019	0.0017	0.002	0.0019	0.0013
40	0.0019	0.0024	0.0029	0.0027	0.0015

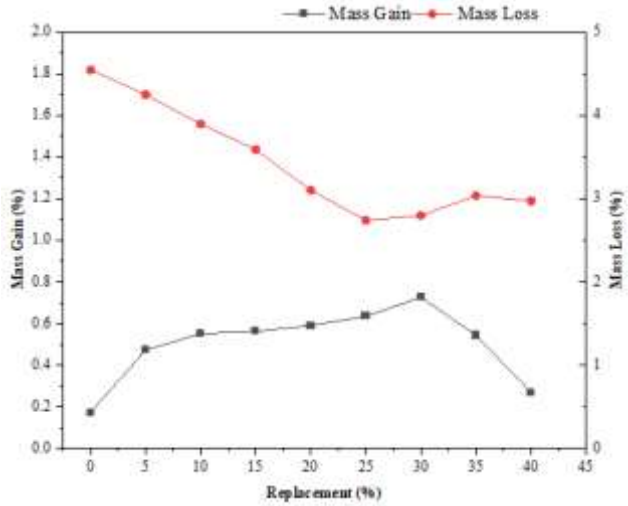

Fig 15. Mass change of the specimens exposed to both sulfate and ambient curing condition.

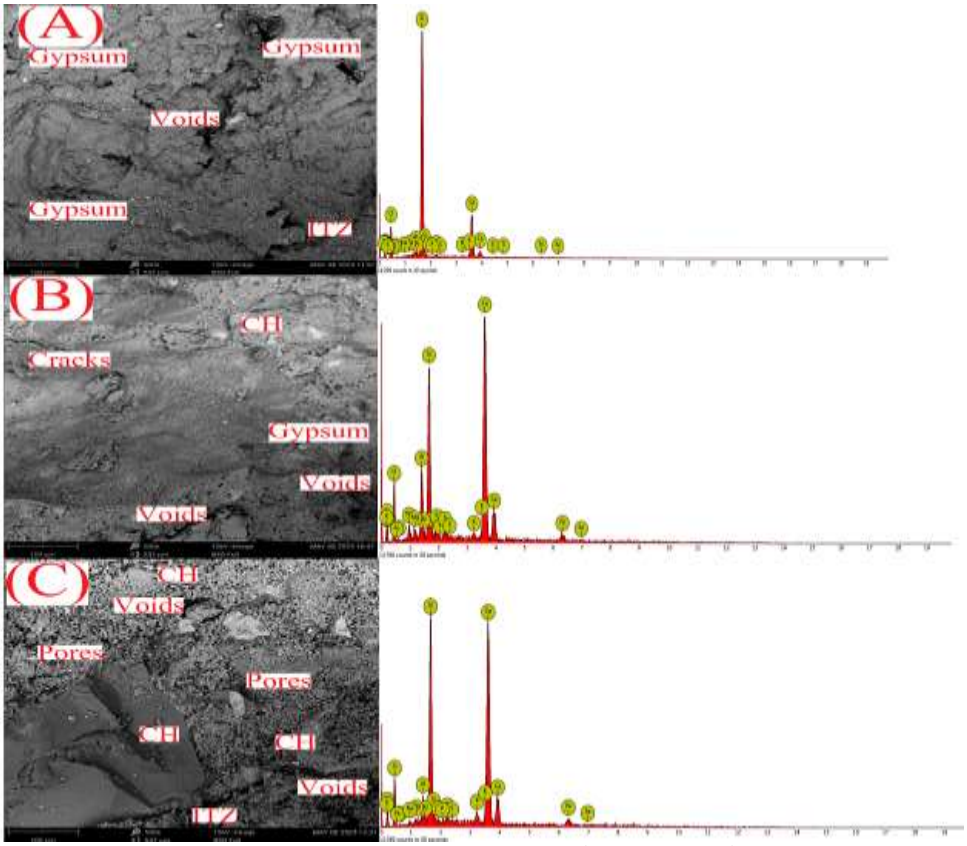

Fig 16. Scanning electron microscopy and energy dispersive x-ray of concrete mixes for mass change at day 365.

As shown in the table 6, the silica-to-aluminium ratio is low mostly in the mixes with fly ash. This is probably as a result of the greater amount of Al and Si that dissolves from the fly ash particles to balance the concentration of the fly ash mix. The dissolution of Si results in a properly formed C-A-S-H structure shown in Figure 16B and 16C.

Table 6. Elemental weight percentage from EDX analysis on mass change at day 365

Element Number	Element Symbol	Control (A) 0%	25% (B) Replacement	40% (C) Replacement
20	Ca	23.36	42.06	36.56
14	Si	35.06	26.32	28.43
26	Fe	8.44	5.32	6.22
13	Al	7.92	7.24	7.51
47	Ag	0.54	0.42	1.6
16	S	12.53	12.41	12.41
19	K	4.78	2.4	3.72
15	P	0.42	0.22	0.22
12	Mg	0.16	0.03	0.06
17	Cl	1.85	1.24	1.64
11	Na	0.34		0.16
22	Ti	2.13	1.34	1.01
8	O			
7	N		0.08	
6	C	1.93	2.19	2.17
	Si/Al	4.4	3.6	3.8
	Na/Al	0.04	-	0.02

Also, the EDXS analysis reveals that more calcium than silica is used in the control mix than in the other mixes, hence the outcome of gypsum when this calcium hydrate (Portlandite) mixes with applied sulfate. The level of deterioration is minimal in the 25% replacement mix in Figure 16B compared to the 40% replacement mix in Figure 16C; there are traces of cracks in both mixes but no visible form of ettringites.

Conclusions: This study provides insights into the use of fly ash in lean concrete production with regard to compressive strength, chloride ion penetration resistance, water absorption, and weight loss at various replacement levels. While the control mix exhibited superior compressive strength, the fly ash mixes demonstrated enhanced durability properties. These findings suggest that incorporating fly ash into lean concrete production can enhance durability without compromising compressive strength.

REFERENCES

Al-Modern, HMJ; ALabedi, THK; Alasadi, LAM (2018). Properties improvement of lean concrete mixes using silica-fume and polymers. *Int J Eng Res Appl*. 9(9): 1418–1424.

ASTM C 39 (2001). Standard Test Method for Compressive Strength of Cylindrical Concrete Specimens. ASTM International, West Conshohocken, PA.

ASTM C1202 (2012). Standard Test Method for Electrical Indication of Concrete's Ability to Resist Chloride. ASTM International, West Conshohocken, PA.

ASTM C136 (2006). Standard Test Method for Sieve Analysis of Fine and Coarse Aggregates. ASTM International, West Conshohocken, PA.

ASTM C1585 (2013). Standard Test Method for Measurement of Rate of Absorption of Water by Hydraulic-Cement Concretes. ASTM International, West Conshohocken, PA.

ASTM C29/C29M (2016). Standard Test Method for Bulk Density and Voids in Aggregate. ASTM International, West Conshohocken, PA.

ASTM C33/C33M (2018). Standard Specification for Concrete Aggregates. ASTM International, West Conshohocken, PA.

ASTM C618 (2019). Standard Specification for Coal Fly Ash and Raw or Calcined Natural Pozzolan for use in Concrete. ASTM International, West Conshohocken, PA.

ASTM D2487 (2017). Standard Practice for Classification of Soils for Engineering Purposes (Unified Soil Classification System). ASTM International, West Conshohocken, PA.

BS 1881-103 (1993). Method for determination of compacting factor. *BSI Standards Institute*.

BS 812-109 (1990). Methods for determination of

moisture content. *British Standards Institute*.

BS 812-110 (1990). Testing aggregates-method for determination of aggregate crushing value (ACV). *British Standards Institute*.

BS 812-112 (1990). Testing aggregates-method for determination of aggregate impact value (AIV). *British Standards Institute*.

BS EN 1008 (2002). Specification for sampling, testing and assessing the suitability of water, including water recovered from processes in the concrete industry, as mixing water for concrete. *British Standards Institute*, *3*, 22.

BS EN 1097-6 (1995). Tests for mechanical and physical properties of aggregates. *British Standards Institute*.

British Standards - BS EN 196-6. (2018). Methods of testing cement-determination of fineness. *British Standards Institute*.

BS EN197-1 (2011). Cement composition, Specifications and conformity criteria for common cements. *British Standards Institute*, 56.

Demir, İ; Güzelkücük, S; Sevim, Ö (2018). Effects of sulfate on cement mortar with hybrid pozzolan substitution. *Int. J. Eng. Sci. Technol*. 21(3): 275–283.

Dillard, R (2021). Comparison of the Resistance of Belitic Calcium Sulfoaluminate Cement and Portland Cement to Sulfate Attack and Sulfuric Acid. May. University of Arkansas. pp.53.

Guo, JJ; Liu, PQ; Wu CL; Wang, K (2021). Effect of dry–wet cycle periods on properties of concrete under sulfate attack. *Appl. Sci.* 11(2): 1–17.

Ikumapayi, CM (2017). Crystal and microstructure analysis of Pozzolanic properties of bamboo leaf ash and locust beans pod ash blended cement concrete. *J. Appl. Sci. Environ. Manage.* 20(4): 943.

Ikumapayi, CM (2018). Properties of groundnut shell (Arachis hypogaea) ash blended portland cement. *J. Appl. Sci. Environ. Manage.* 22(10): 1553.

Ikumapayi, CM (2019). Development of a short time model for predicting chloride ingress into normal and pozzolanic concrete. *IOP Conf. Ser.: Mater. Sci. Eng*. 640(1): 012113

Jaya, RP (2020). Porous concrete pavement containing nanosilica from black rice husk ash. *J. Mater. Civ. Eng*. 3(4): 493-527

Jemimah, CM; Prince, AG (2019). Rapid chloride permeability test on concrete with nano materials. *Int J Eng Adv Technol*. 8(3): 103–109.

Kotwa, A (2015). Effect of selected admixtures on the properties of ordinary concrete. *Procedia Eng*. Vol. 108: 504–509.

Liu, K; Sun, D; Wang, A; Zhang, G; Tang, J (2018). Long-Term Performance of Blended Cement Paste Containing Fly Ash against Sodium Sulfate Attack. *J. Mater. Civ. Eng*. 30(12): 1–10.

Liu, Z; Liu, G; Zhang, G (2022). Effect of Curing Time on the Surface Permeability of Concrete with a Large Amount of Mineral Admixtures. *Adv. Civ. Eng.* Vol. 2022. ISSN 1687-8094.

Malkawi, AB; Nuruddin, MF; Fauzi, A; Almattarneh, H; Mohammed, BS (2016). Effects of alkaline solution on properties of the HCFA geopolymer mortars. *Procedia Eng*. 148(10): 710–717.

Nath, P; Sarker, P (2011). Effect of fly ash on the durability properties of high strength concrete. *Procedia Eng*. Vol. 14: 1149–1156.

Nwokocha, P; Munachiso, O (2022). Analysis on chemical composition of different brands of cement in Nigeria with their corresponding setting Time. *Int. J. Res. Sci. Innov. Appl. Sci*. 7(4): 45–50.

Pati, SL; Kale, JN; Suman, S (2003). Fly Ash Concrete : A technical analysis for compressive strength. *Int. J. adv. eng. res. stud*. 2(1): 4–5.

Rukzon, S; Chindaprasirt, P (2014). Use of Ternary Blend of Portland Cement and Two Pozzolans to Improve Durability of High-strength Concrete. *KSCE J. Civ. Eng.* 18(6): 1745–1752.

Saha, AK (2018). Effect of class F fly ash on the durability properties of concrete. *Sustain. Environ. Res.* 28(1): 25–31.

Siddique, R (2004). Performance characteristics of high-volume Class F fly ash concrete. *Cem. Concr. Res.* 34(3): 487–493.

Sudheen, A (2008). Sulfate and Alkali Silica Resistance of Class C and F Fly Ash Replaced

Blended Cements. Arizona State University. pp. 1-135

Sumer, M (2012). Compressive strength and sulfate resistance properties of concretes containing Class F and Class C fly ashes. *Constr. Build. Mater.* Vol. 34: 531–536.

Verapathran, M; Murthia, P (2016). Acid resistance and rapid chloride permeability of high performance concrete. *Int. J. Chem. Sci.* 14(2): 1015–1025.

von Fay, KF (1995). Effects of Various Fly Ashes on Compressive Strength, Resistance to Freezing and Thawing, Resistance to Sulfate Attack, and Adiabatic Temperature Rise of Concrete.

Wilińska, I; Pacewska, B (2018). Influence of selected activating methods on hydration processes of mixtures containing high and very high amount of fly ash. *J. Therm. Anal. Calorim.* 133(1): 823–843.

Zhang, Q; Xi, B (2016). Analysis of Testing Methods for Chloride Ion Permeability in Marine Concrete. *IFEESD*. pp.55–62. ISSN 2352-5401